



## Long-range magnetic order in CeRu<sub>2</sub>Al<sub>10</sub> studied via muon spin relaxation and neutron diffraction

D. D. Khalyavin,<sup>1</sup> A. D. Hillier,<sup>1</sup> D. T. Adroja,<sup>1</sup> A. M. Strydom,<sup>2</sup> P. Manuel,<sup>1</sup> L. C. Chapon,<sup>1</sup> P. Peratheepan,<sup>2</sup> K. Knight,<sup>1</sup> P. Deen,<sup>3</sup> C. Ritter,<sup>3</sup> Y. Muro,<sup>4</sup> and T. Takabatake<sup>4</sup>

<sup>1</sup>ISIS Facility, Rutherford Appleton Laboratory, STFC, Chilton, Didcot, Oxfordshire OX11 0QX, United Kingdom

<sup>2</sup>Physics Department, University of Johannesburg, P.O. Box 524, Auckland Park 2006, South Africa

<sup>3</sup>Institute Laue-Langevin, 6 Rue Jules Horowitz, BP 156, 38042 Grenoble Cedex 9, France

<sup>4</sup>Department of Quantum Matter, ADSM, and IAMR, Hiroshima University, Higashi-Hiroshima 739-8530, Japan

(Received 8 June 2010; published 7 September 2010)

The low-temperature state of CeRu<sub>2</sub>Al<sub>10</sub> has been studied by neutron powder diffraction and muon spin relaxation. By combining both techniques, we prove that the transition occurring at  $T^* \sim 27$  K, whose origin has been the subject of considerable debate, is unambiguously magnetic due to the ordering of the Ce sublattice. The magnetic structure with a propagation vector of  $\mathbf{k}=(1,0,0)$  involves a collinear antiferromagnetic alignment of the Ce moments along the  $c$  axis of the  $Cmcm$  space group with a reduced moment of  $0.34(2) \mu_B$ . No structural changes within the resolution limit have been detected below the transition temperature. However, the temperature dependence of the magnetic Bragg peaks and the muon precession frequency show an anomaly around  $T_2 \sim 12$  K indicating a possible second transition.

DOI: [10.1103/PhysRevB.82.100405](https://doi.org/10.1103/PhysRevB.82.100405)

PACS number(s): 71.27.+a, 61.05.F–, 75.30.Mb

A phase transition recently discovered in the orthorhombic heavy fermion compound CeRu<sub>2</sub>Al<sub>10</sub> has attracted great attention due to the possible unconventional physics behind it.<sup>1</sup> Initially, the transition was attributed to magnetic ordering of the cerium moments,<sup>1</sup> based on macroscopic measurements which revealed pronounced anomalies in various physical properties. However, the unexpectedly high critical temperature ( $T^* \sim 27$  K) and magnetic-susceptibility data obtained for different crystallographic directions,<sup>2</sup> as well as <sup>27</sup>Al nuclear quadrupole resonance/NMR measurements<sup>3</sup> raised doubts about the magnetic nature of this transition. Several alternative interpretations have recently been proposed<sup>2–4</sup> but the most popular scenario involves the formation of a spin-singlet state of Ce suggested by Tanida *et al.*<sup>4</sup> This would correspond to an effective reduction in dimensionality of the system due to structural distortions, namely, a spin-Peierls transition.<sup>5</sup> This idea was backed up by recent neutron-scattering experiments revealing a possible superstructure below  $T^*$  and the presence of low-energy modes interpreted as singlet-triplet excitations from dimerized Ce ions.<sup>6</sup> The origin of the superstructure reflections was however not clarified experimentally until the recent theoretical work by Hanzawa<sup>7</sup> attributing them to displacements of some Al sites with an associated symmetry lowering from  $Cmcm$  down to  $Pmnn$ . Understanding the origin of the superstructure reflections is obviously key to determining the ground state of CeRu<sub>2</sub>Al<sub>10</sub> and should allow for a quantitative analysis of the order parameter at the phase transition.

In the present communication, we show by combining the results of muon spin relaxation ( $\mu^+$ SR) and powder neutron diffraction that the transition at  $T^*$  is magnetic in origin and involves long-range order of the Ce moments. Below  $T^*$ , the observation in the neutron data of several superlattice reflections not detected previously<sup>6</sup> and indexed by the propagation vector  $\mathbf{k}=(1,0,0)$  enables a full analysis of the magnetic configuration. The refinements of the data show that the best

model corresponds to an antiferromagnetic order of the Ce moment along the  $c$  axis of the  $Cmcm$  space group. The data cannot be explained by magnetic ordering of the Ru sublattice or by a structural transition and is uniquely compatible with one of the symmetry modes calculated for the Ce site. The reduction in paramagnetic background below  $T^*$  in the neutron data and the independent observation of coherent oscillations due to internal field in the  $\mu^+$ SR confirms the magnetic origin of the transition. Anomalies detected primarily in the  $\mu^+$ SR data indicate that additional transitions, which origins are not yet understood, appear below  $T^*$ .

A polycrystalline sample of CeRu<sub>2</sub>Al<sub>10</sub> used in the powder neutron diffraction and zero-field muon spin-relaxation experiments was prepared by ultrahigh-purity argon arc melting of stoichiometric quantities of the starting elements. Both experiments were carried out at the ISIS pulsed neutron and muon source of the Rutherford Appleton Laboratory, U.K., on the MuSR spectrometer and WISH diffractometer on the second target station (TS-2). The  $\mu^+$ SR experiments were conducted in longitudinal geometry. The powdered sample was mounted onto a 99.995+% pure silver plate. The sample and mount were then inserted into a cryostat with a temperature range of 1.2–300 K. Muons implanting into any exposed part of the silver mount give rise to a flat time-independent background. For the neutron-diffraction experiment, a 6 g sample was loaded into a cylindrical 6 mm vanadium can and placed in an Oxford instrument cryostat. Data were recorded in the temperature interval 1.5–30 K, with long counting times (8 h) at  $T=1.5$  K and  $T=30$  K. Intermediate temperature points were measured with a lower exposition time ( $\sim 2$  h). The program FULLPROF (Ref. 8) was used for Rietveld refinements and group-theoretical calculations were performed with the aid of the ISOTROPY software.<sup>9</sup>

The neutron-diffraction patterns collected at  $T > T^*$  are consistent with the  $Cmcm$  symmetry and can be satisfactorily fitted ( $R_{Brag}=4.95\%$ ) with the structural model proposed by

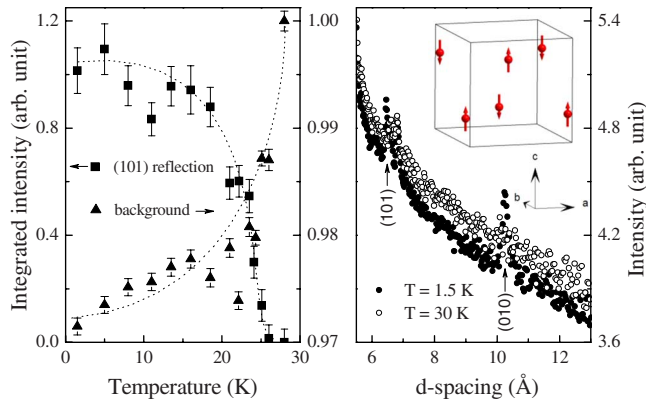


FIG. 1. (Color online) Integrated intensity of the (101) reflection and the background as a function of temperature (left panel). Dotted lines are a guide to the eye. A low- $Q$  region of two diffraction patterns collected at  $T=1.5$  K and  $T=30$  K (right panel). The inset shows ordering of Ce magnetic moments at  $T=1.5$  K.

Thiede *et al.*<sup>10</sup> From our refinements, the unit-cell parameters at  $T=30$  K are  $a=9.1322(2)$  Å,  $b=10.2906(2)$  Å, and  $c=9.1948(2)$  Å. Below  $T^*$ , a set of new reflections (Fig. 1) associated with the  $\mathbf{k}=(1,0,0)$  propagation vector (Y point of symmetry in Miller and Love notations<sup>11</sup>) appears indicating the phase transition detected in previous investigations by numerous experimental techniques.<sup>1–4</sup> These reflections are only clearly visible at low-momentum transfer ( $Q$ ) while there is no detectable change at high  $Q$ . By taking the difference between the patterns collected at  $T=1.5$  K and  $T=30$  K, seven peaks with intensities significantly higher than the error bars and  $d$  spacing  $>3$  Å [Fig. 2 (top)] can be identified. Another important feature is the reduction in the background observed at low  $Q$  and concomitant with the appearance of the superlattice reflections below  $T^*$  (Fig. 1). Once again, this is consistent with the existence of a magnetic transition below which the intensity contained in the paramagnetic scattering is suppressed and transferred to Bragg scattering. This is best seen in the temperature dependence of the integrated intensity of the strongest superlattice peak (101) and the background integrated in the range 7–10 Å shown in Fig. 1 (left).

To obtain an appropriate model for the magnetic structure, we employed a method whereby combinations of axial vectors localized on the  $4c$ (Ce) and  $8d$ (Ru) sites and transforming as basis functions of the irreducible representations (irreps) of the wave-vector group [ $\mathbf{k}=(1,0,0)$ ], are systematically tested.<sup>12</sup> In agreement with the Landau theory of continuous transition, we found that a single irrep is involved. A unique solution ( $R_{nuc1}=4.72\%$  and  $R_{mag}=14.65\%$ ) associated with the  $Y_3^-$  irrep was found assuming magnetic ordering of the Ce sublattice (Fig. 2). None of the magnetic modes spanned by a single irrep for the  $8d$ (Ru) sites was able to fit the data properly. This is consistent with the absence of a transition in the isostructural compound  $\text{LaRu}_2\text{Al}_{10}$ .<sup>4,10</sup> The obtained model consists of collinear antiferromagnetic ordering of the Ce moments aligned along the  $c$  axis of the  $Cmcm$  space group [Fig. 1 (inset) and Fig. 2 (bottom)]. The antiparallel configuration is adopted by the ions related by the glide plane and the centering lattice trans-

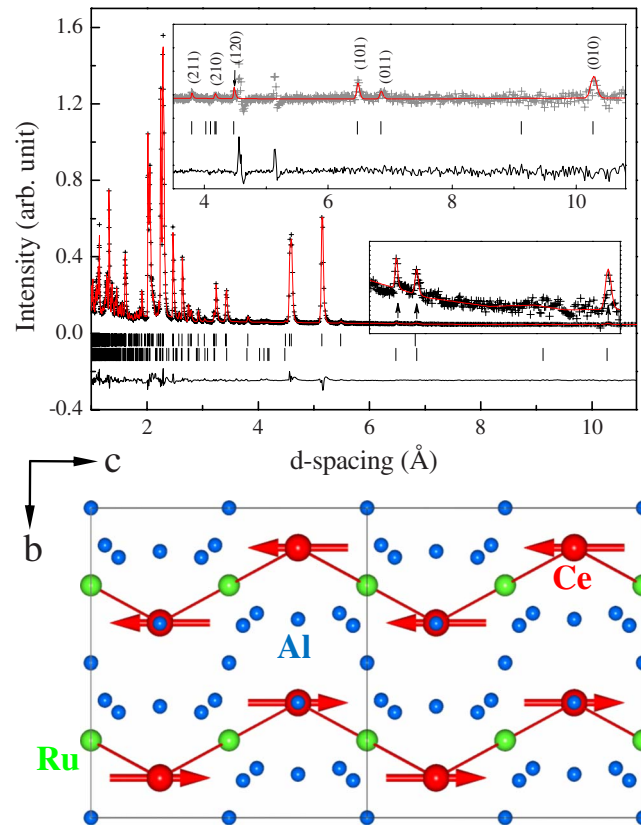


FIG. 2. (Color online) Rietveld refinement of the neutron powder-diffraction pattern obtained at 1.5 K. The cross symbols and (red) solid line represent the experimental and calculated intensities, respectively, and the line below is the difference between them. Tick marks indicate the positions of Bragg peaks for the nuclear scattering ( $Cmcm$  space group, top line) and magnetic scattering [ $\mathbf{k}=(1,0,0)$  propagation vector, bottom line]. The inset shows the refinement of the pure magnetic scattering, obtained by taking the difference between data sets at 1.5 and 30 K. The asymmetric features are due to slight differences in  $d$  spacing of the nuclear peaks at different temperatures (thermal expansion). Bottom panel: schematic representation of the magnetic structure of  $\text{CeRu}_2\text{Al}_{10}$ , projected onto the  $(bc)$  plane

lation. The latter comes directly from the propagation vector which is  $\mathbf{k}=(1/2,1/2,0)$  with respect to the primitive unit cell. The corresponding magnetic space group is  $C_p m' cm$  (number 63.11.521 in the Litvin's classification scheme).<sup>13</sup> The refined value of the Ce magnetic moment is  $0.34(2)$   $\mu_B$  at  $T=1.5$  K and its temperature dependence varies as the square root of the integrated intensity of the (101) reflection [Fig. 1 (left)]. A small anomaly around  $T_2 \sim 12$  K possibly indicates an additional transition but data on single crystal would be necessary to determine the exact nature of this transition. We note that this anomaly is also observed in the  $\mu^+$ SR data discussed below.

An alternative explanation for the transition below  $T^*$ , which is widely discussed in the literature, is the dimerization of Ce, i.e., a spin-Peierls transition where the formation of a spin-gapped singlet state drives a structural modulation. Several space groups were proposed based on different experiments<sup>3</sup> and theoretical considerations.<sup>7</sup> Our analysis

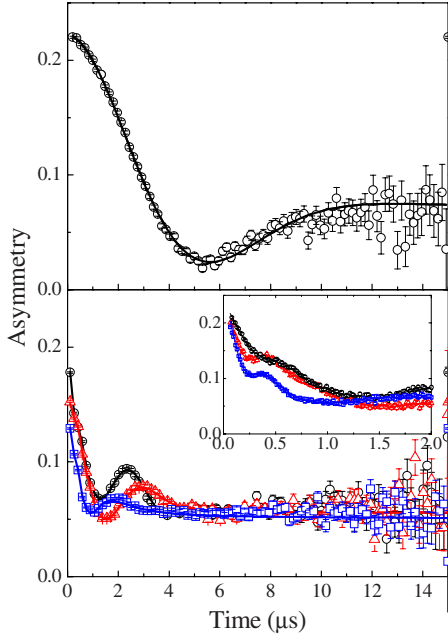


FIG. 3. (Color online) The upper graph shows the muon depolarization spectrum at 30 K. The line is a least-squares fit to the data using Eq. (2). The lower graph shows muon depolarization spectra for a range of temperatures [namely, 1.4 K (blue) squares, 10.8 K (red) triangles, and 23.0 K (black) circles]. The inset shows the same data at shorter times. In both cases, the line is a least-squares fit to the data using Eq. (3).

does not support this model. First of all, qualitatively, one would expect in such a case that the superstructure reflections observed by neutron diffraction would be present at high-momentum transfer since their intensity would not be modulated by the magnetic form factor. In addition, at such low temperatures, the intensity is not damped by high thermal parameters. Second, it appears that a structural distortion can be discarded by a quantitative analysis: the only isotropy subgroup associated with the  $Y$ -symmetry point that can account for all observed superstructure reflections is  $Pm\bar{m}n$ . An unconstrained refinement with this symmetry was unstable and therefore another approach based on symmetry-adapted atomic displacements was employed. Considering all atoms in the unit cell (Ce, Ru, and Al), there are 11 modes with the  $Y_4^-$  symmetry that can act as primary order parameters at the  $Cmcm \rightarrow Pm\bar{m}n$  displacive phase transition. All these modes were introduced in the refinement either independently or combined but none gave a significant contribution to the observed superstructure peaks, further confirming their magnetic origin. It should be pointed out however that this result does not imply that the symmetry of the low-temperature phase is necessarily  $Cmcm$  nor does it preclude the presence of very weak secondary structural modes beyond the sensitivity of our measurements.

Further arguments in favor of long-range magnetic order are obtained from  $\mu^+$ SR measurements. The muon spin relaxation for a metallic system that does not exhibit magnetic order will only be sensitive to the local fields associated with the nuclear spins. Normally, on the time scale of the muon, these nuclear spins are static and randomly orientated. There-

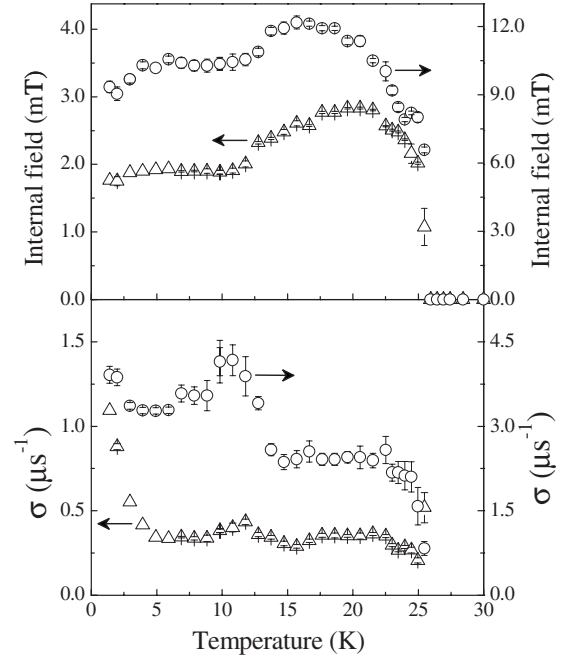


FIG. 4. Temperature dependences of the internal field (upper graph) and the muon depolarization rate (lower graph) at the muon sites. For both graphs, the  $\Delta$  are associated with the left axis while the  $\circ$  are associated with the right axis.

fore, the  $\mu^+$ SR spectra can be described by the Kubo-Toyabe function<sup>14</sup>

$$G_z^{KT}(t) = \left[ \frac{1}{3} + \frac{2}{3}(1 - \Delta^2 t^2) \exp\left(-\frac{\Delta^2 t^2}{2}\right) \right], \quad (1)$$

where  $\Delta/\gamma_\mu$  is the local-field distribution width and  $\gamma_\mu/2\pi = 135.5$  MHz/T is the muon gyromagnetic ratio. In the magnetically ordered state, the muon polarization will precess with a frequency which is directly proportional to the ordered moment. The spectra above the phase-transition temperature ( $T^* \sim 27$  K) are best described [see Fig. 3 (top)] by

$$G_z(t) = A_0 G_z^{KT}(t) \exp(-\lambda t) + A_{bck}, \quad (2)$$

where  $\lambda$  is the relaxation rate associated with the dynamic electronic spin fluctuations. As the transition at  $\sim 27$  K is approached, from above, there is a slight increase in the  $\lambda$  term whereas  $\Delta$  remains temperature independent ( $\Delta = 0.30 \mu\text{s}^{-1}$ ). This increase in  $\lambda$  is indicative of the approach to a magnetic transition. As the temperature is further decreased, the  $\mu^+$ SR spectra clearly show the presence of coherent oscillations. The presence of these oscillations with one frequency has been previously reported,<sup>15</sup> however, our analysis shows that there are at least two precession frequencies [see Fig. 3 (bottom and inset)], which is consistent with our  $\mu^+$ SR results on CeOs<sub>2</sub>Al<sub>10</sub> (Ref. 16) and indeed our spectra are well described using the following equation:

$$G_z(t) = \sum_{i=1}^2 A_{o,i} \exp(-\sigma_i^2 t^2/2) \cos(\gamma_\mu B_i t + \varphi) + A_{r,i} \exp(-\lambda_i t) + A_{bck}, \quad (3)$$

where  $B_i$  is the internal field,  $\sigma_i$  is the depolarization rate,  $\lambda_i$  is, again, the spin fluctuations along the  $z$  direction,  $\varphi$  is the phase of the oscillations, and finally  $A_{bck}$  is the background. The value of  $A_{bck}$  was determined from the spectra above the transition temperature and fixed for all the fits below. Figure 4 shows the temperature dependence of the internal field and the depolarization rate. These results clearly indicate the appearance of precession in the  $\mu^+$ SR spectra below  $\sim 27$  K. Furthermore, examination of the amplitudes of the oscillating term leads to the conclusion that the sample is fully magnetically ordered. The temperature evolution of the internal fields shows a rapid increase in both frequencies below  $T^* \sim 27$  K, followed by a broad hump around 20 K, and a plateau between 5 and 12 K. Below 5 K, a small decrease in the internal field is observed. The depolarization rates also display a broad hump close to 20 K, similar to that observed for the internal fields. Interestingly, there is a peak in  $\sigma_i$  at  $T_2 \sim 12$  K which also coincides with the anomaly in the temperature dependence of the integrated intensity of the (101) magnetic peak [see Fig. 1 (left)] and possibly indicates an additional phase transition.

Thus, both the  $\mu^+$ SR data and neutron-diffraction measurements unequivocally point to the existence of a long-range magnetic order in  $\text{CeRu}_2\text{Al}_{10}$ . The origin of the high critical temperature and low value of the ordered moment is

not clear at present and requires further experimental and theoretical efforts. The latter can be possibly related to a particularly strong hybridization between Ce  $4f$  and conduction electrons. The high ordering temperature is difficult to attribute to Ruderman-Kittel-Kasuya-Yoshida interactions only. In this respect, an important observation is the lack of transition in the isostructural compound  $\text{CeFe}_2\text{Al}_{10}$ .<sup>10</sup> This emphasizes the significant role played by the Ru sublattice in transmitting interactions between the well-separated Ce ions [Fig. 2 (bottom)]. The main difference between Fe and Ru is the diffuseness of the outer electronic shells ( $5p/5d$  versus  $4p/4d$ ) whose effect will need to be investigated by *ab initio* calculations in the light of our experimental finding.

In conclusion, the orthorhombic compound  $\text{CeRu}_2\text{Al}_{10}$  exhibits a phase transition at  $T^* \sim 27$  K associated with long-range magnetic ordering of the Ce sublattice. The propagation vector of the ordered state is  $\mathbf{k}=(1,0,0)$  and does not change with temperature. The magnetic structure at  $T=1.5$  K involves a collinear antiferromagnetic orientation of the Ce moments along the  $c$  axis of the  $Cmcm$  space group with a magnitude of  $0.34(2) \mu_B$ . The small value of the magnetic moments is not related to the presence of a disordered component and is an intrinsic property of the fully ordered state. Around  $T_2 \sim 12$  K a possible structural/magnetic phase transition takes place as evidenced by the anomalous behavior of the muon depolarization rate and precession frequencies.

A. M. Strydom and P. Peratheepan thank Faculty Research Committee of UJ and the SA-NRF (2072956) for financial support.

<sup>1</sup>A. M. Strydom, *Physica B* **404**, 2981 (2009).

<sup>2</sup>T. Nishioka, Y. Kawamura, T. Takesaka, R. Kobayashi, H. Kato, M. Matsumura, K. Kodama, K. Matsubayashi, and Y. Uwatoko, *J. Phys. Soc. Jpn.* **78**, 123705 (2009).

<sup>3</sup>M. Matsumura, Y. Kawamura, S. Edamoto, T. Takesaka, H. Kato, T. Nishioka, Y. Tokunaga, S. Kambe, and H. Yasuoka, *J. Phys. Soc. Jpn.* **78**, 123713 (2009).

<sup>4</sup>H. Tanida, D. Tanaka, M. Sera, C. Moriyoshi, Y. Kuroiwa, T. Takesaka, T. Nishioka, H. Kato, and M. Matsumura, *J. Phys. Soc. Jpn.* **79**, 043708 (2010).

<sup>5</sup>K. Hanzawa, *J. Phys. Soc. Jpn.* **79**, 043710 (2010).

<sup>6</sup>J. Robert, J. Mignot, G. André, T. Nishioka, R. Kobayashi, M. Matsumura, H. Tanida, D. Tanaka, and M. Sera, *Phys. Rev. B* **82**, 100404(R) (2010).

<sup>7</sup>K. Hanzawa, *J. Phys. Soc. Jpn.* **79**, 084704 (2010).

<sup>8</sup>J. Rodríguez-Carvajal, *Physica B* **192**, 55 (1993).

<sup>9</sup>H. T. Stokes, D. M. Hatch, and B. J. Campbell, [isotropy.stokes.byu.edu/isotropy.html](http://isotropy.stokes.byu.edu/isotropy.html) (2007).

<sup>10</sup>V. M. T. Thiede, T. Ebel, and W. Jeitschko, *J. Mater. Chem.* **8**, 125 (1998).

<sup>11</sup>S. C. Miller and W. F. Love, *Tables of Irreducible Representations of Space Groups and Co-Representations of Magnetic Space Groups*, 4th ed. (Prentice Hall, Englewood Cliffs, 1967).

<sup>12</sup>Yu. A. Izumov, V. E. Naish, and R. P. Ozerov, *Neutron Diffraction of Magnetic Materials* (Consulting Bureau, New York, 1991).

<sup>13</sup>D. B. Litvin, *Acta Crystallogr., Sect. A: Found. Crystallogr.* **64**, 419 (2008).

<sup>14</sup>R. S. Hayano, Y. J. Uemura, J. Imazato, N. Nishida, and T. Yamazaki, *Phys. Rev. B* **20**, 850 (1979).

<sup>15</sup>S. Kambe, H. Chudo, Y. Takunaga, T. Koyama, H. Sakai, T. U. Ito, K. Ninomiya, W. Higemoto, T. Takesaka, T. Nishioka, and Y. Miyake, *J. Phys. Soc. Jpn.* **79**, 053708 (2010).

<sup>16</sup>D. T. Adroja, A. D. Hillier, P. P. Deen, A. M. Strydom, Y. Muro, J. Kajino, W. A. Kockelmann, T. Takabatake, V. K. Anand, J. R. Stewart, and J. Taylor, *Phys. Rev. B* **82**, 104405 (2010).